AIAA JOURNAL
Vol. 39, No. 4, April 2001

Model Development and Analysis of the Dynamics of Pressure-Sensitive Paints

Neal A. Winslow,* Bruce F. Carroll,† and Andrew J. Kurdila‡
University of Florida, Gainesville, Florida 32611-6250

Two models for the dynamic behavior of pressure-sensitive paints are developed. The first of the two models is a purely empirical approach to designing a model and compensator. The second model presented encompasses the physics of the process by which an unsteady pressure field over the paint layer affects the layer and causes an intensity of fluorescence that is fluctuating in time. Within this second model, two different forms for the static calibration are chosen. The effect of the calibration on the system dynamics is demonstrated.

Nomenclature

A	=	amplitude
a	=	pressure-sensitive paint thickness
b	=	intercept of linear Stern–Volmer static calibration
c	=	calibration constants
D	=	diffusivity
E	=	activation energy
f	=	calibration function from pressure to intensity
g	=	calibration function from intensity to pressure
H	=	transfer function
I	=	integrated intensity
J	=	intensity per unit thickness
j	=	the complex number, $\sqrt{-1}$
K	=	intensity error per unit thickness relative to surface condition
M	=	model order
m	=	oxygen concentration difference relative to surface condition
n	=	oxygen concentration
P	=	pressure
T	=	temperature
t	=	time
x	=	distance from substrate
α	=	modal states
λ	=	eigenvalues
σ	=	solubility
τ	=	time constant
ϕ	=	phase
Ψ	=	spatial eigenfunctions
ω	=	frequency

Superscripts and Subscripts

$\tilde{H}$	=	Fourier transform of H
$\dot{H}$	=	time derivative of H
in	=	input
out	=	output
model	=	model output
ref	=	at reference conditions
$*$	=	dimensionless
0	=	initial
1	=	final
0.xx	=	at xx% response (e.g., 0.99)

Received 30 December 1999; revision received 5 July 2000; accepted for publication 7 July 2000.

*Graduate Student, Department of Aerospace Engineering, Mechanics and Engineering Science. Student Member AIAA.

†Associate Professor, Department of Aerospace Engineering, Mechanics and Engineering Science. Member AIAA.

‡Professor, Department of Aerospace Engineering, Mechanics and Engineering Science. Member AIAA.

Introduction

PRESSURE-SENSITIVE paint (PSP) has been an emergent technology during the past 5–10 years. Many different groups have made contributions as is summarized in the reviews by McLachlan and Bell[1] and Liu et al.[2] Much success has been achieved in the application of PSP to steady pressure fields. In comparison, there are but a few papers discussing the application of PSP to unsteady pressure fields. This paper presents a physically realistic model for the dynamic response of PSPs and provides a foundation for further development of dynamic compensation schemes for PSP data analysis.

PSP is a measurement technique that has its roots in photochemistry. It is based on the fluorescence quenching effect of oxygen on luminescent molecules in a polymer binder. As such, the earliest reference of this phenomenon in unsteady situations comes from polymer chemistry. Cox and Dunn[3] wrote a paper that has the beginnings of a good model for the response of PSP to unsteady pressure fields. They investigated oxygen transport within poly(dimethyl siloxane) (PDMS) via its effect on the fluorescence of the luminophor 9,10-diphenyl anthracene. The purpose of their work was to determine such physical quantities as the solubility, diffusivity, and activation energies of the polymer PDMS. They accomplished this with a cuvette ($a = 1$ cm) of PDMS into which was mixed the luminophor 9,10-diphenyl anthracene. A schematic of a typical PSP is shown in Fig. 1 and is similar to the geometry of the cuvette used in their experiments. The cuvette was allowed to come to equilibrium with pure nitrogen at 1 atm. Then the nitrogen environment was replaced with pure oxygen at 1 atm. Over the next 24 hours, the fluorescence intensity at the center of the cuvette ($x = 4.5$–5.5 mm) was monitored. The fluorescence intensity was seen to fall off quasi-exponentially. With the use of a static calibration, they were able to back out the indicated oxygen concentration as a function of time within the PDMS. They then developed an analytical model for the indicated oxygen concentration using the one-dimensional diffusion equation. For a step change in oxygen concentration at the upper surface ($x = a$) the analytical solution for the oxygen concentration within the cuvette is

$$\frac{n(x,t)-n_0}{n_1-n_0} = 1 - \frac{4}{\pi}\sum_{m=0}^{\infty}\left(\frac{1}{2m+1}\right) \times \exp\left[-(2m+1)^2\frac{\pi^2}{4}\frac{Dt}{a^2}\right]\sin\left[(2m+1)\frac{\pi}{2}\frac{x}{a}\right] \tag{1}$$

This model was found to accurately represent the experimental data. The regression analysis yielded values of diffusivity between $D = 2.0 \times 10^{-5}$ cm^2/s at $T = 5^\circ$C and $D = 6.1 \times 10^{-5}$ cm^2/s at $T = 45^\circ$C for oxygen in PDMS. However, in the general use of PSPs, the coating is viewed from above rather than from the side. That is, the intensity measured from a PSP is the integrated intensity of the entire layer. The integrated intensity as a function of time for

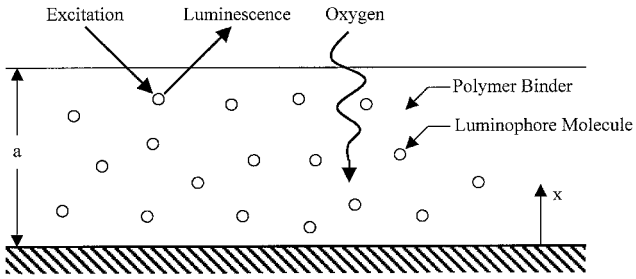

Fig. 1 Schematic of a typical PSP layer.

an arbitrary unsteady pressure field will be shown later to have a troublesome nonlinearity.

Perhaps the first true example of unsteady PSP was by Baron et al.[4] Here, the inverse of the PSP intensity was compared to the pressure as the pressure was quickly stepped from near vacuum up to 1atm of standard air. The assumption was made that the PSP responded as a first-order dynamical system with up to two time constants. The given dynamical system was numerically convolved with the pressure signal from a fast conventional transducer to yield a pressure that was compared to the pressure indicated by the PSP. Via nonlinear least-squares curve fitting, the time constants and term weights were determined, yielding an empirical model for the dynamic response of the PSPs. With these empirical models, Baron et al. were able to get extremely good comparisons between their curve fits and their experimental data. This paper was the first attempt at characterizing the dynamics of PSP and used a time domain-based technique.

The work of Borovoy et al.[5] was the first actual wind tunnel application of PSP in unsteady conditions found in the literature. In this experiment the pressure on a cylinder in Mach 6 flow was investigated. To achieve the Mach 6 flow, the cylinder was located perpendicular to the exit of a shock tube. It is stated that the 99% relaxation time of a PSPs fluorescence is given by the equation

$$t_{0.99} = (12/\pi^2)(a^2/D) \tag{2}$$

Once the shock had passed the cylinder, the timing system in the experiment would wait an amount of time given in Eq. (2) and then trigger a single flash from a xenon flash lamp. The PSP data were compared to an analytical solution of Euler's equations for nonviscous flow and found to agree to within 10%. It should be noted that this application was not truly an example of unsteady PSP, as the data were taken after the shock had already passed the cylinder and the PSP had been given sufficient time to respond to the step change in pressure. That is, the flow field was unsteady in time but not during the period over which the data were acquired.

In separate but concurrent developments, the response of PSP to periodic pressure fields was investigated by Engler[6] and Carroll et al.[7] In Engler's work, the PSP was subjected to periodic forcing at frequencies from 0.1 Hz to 50 Hz. The main goal of this investigation was the characterization of the dynamic range and the pressure resolution of the PSP. No effort was made here to perform dynamic compensation or to try to mathematically or physically define the dynamics of the PSP system. Carroll et al. presented experiments similar in form to those of Engler, namely, the response of PSP to sinusoidal pressure fields. Much of the analysis performed here was done in the frequency domain. It was shown that the PSP responds as approximately a first-order dynamic system based on the amplitude response. The phase response of the PSP system did not match well to the standard first-order system model.

Carroll et al.[8] investigated the response of PSP to a step change in pressure. In this paper are the beginnings of a physically realistic model for the dynamic response of PSP to a step change in pressure level. The basics of the paper are that an analytical model was developed on the basis of the one-dimensional mass diffusion equation to describe the transport of oxygen within the PSP layer. This model was nonlinear and was implemented numerically. In addition, empirical models based on a single-term first-order response and on a two-term first-order response were developed. With the use of nonlinear least-squares curvefitting, the two empirical models were fit to the data. The single-term first-order model was shown to inadequately fit the data. The two-term and diffusion-based models were both shown to have excellent agreement with the experimental data. An equivalent form of the diffusion-based model will be derived in its entirety in a later section.

The final paper to be discussed here was from Hubner et al.[9] Pressure and temperature measurements were made on an elliptic cone model in Mach 7.5 flow. The tests were performed at the 48-inch hypersonic shock tunnel at Calspan–University of Buffalo Research Center. Because of the short duration of the flow, a method similar to that of Borovoy et al.[5] was used, wherein the PSP was allowed to come to equilibrium with the flow, and then a photographic strobe was used to illuminate the paint. The data showed that the pressure on the surface of the model ranged from 3 to 12 kPa. A second set of tests was performed with a high frame-rate, eight-bit camera. In these tests the camera acquired several images of a temperature-sensitive paint coated model during a single flash from the strobe. The temperature data from these tests were used to compute heat transfer rates on the surface of the model. The results compared well with measurements made with thin-film heat transfer transducers.

As can be seen in the literature to date, there is a lack of understanding of the fundamental dynamic response of PSPs. It is the goal of this paper to present sound mathematical and physical models for PSP dynamics.

PSP Model Development

The most important step in performing a dynamic analysis of PSP data is in model selection. What follows are two different approaches yielding models increasing in design complexity and accuracy. The first approach is purely empirical in nature. The second is based on solving the one-dimensional mass diffusion equation in conjunction with the relation between intensity and pressure under static conditions.

Empirical Models

Perhaps the easiest model that can be developed is one that does not even attempt to understand the physics of the system in question but rather simply measures the input and output of the system and uses the data as the characterization. This approach is often referred to as the "black box" approach. All one must do is define the input/output mapping for the system as a function of frequency to create a crude compensator to correct for the amplitude damping and phase-shifting behavior. The only underlying assumptions to this type of model are that the system being modeled must be linear and time-invariant. That is, for an input given by

$$P_{\text{in}}(t) = P_0 + P_1 \sin(\omega t) \tag{3}$$

the output from the system must be of the form

$$P_{\text{out}}(t) = P_0 + P_1 A(\omega) \sin(\omega t + \phi(\omega)) \tag{4}$$

In the above equation, A and ϕ are the amplitude ratio and phase shift, respectively, of the output relative to the input and are functions of the driving frequency ω. Equations (3) and (4) can be more easily related to one another in the frequency domain via

$$\tilde{P}_{\text{out}}(j\omega) = \tilde{H}(j\omega)\tilde{P}_{\text{in}}(j\omega) = A(\omega)e^{-j\phi(\omega)}\tilde{P}_{\text{in}}(j\omega) \tag{5}$$

Shown in Fig. 2 on the basis of input/output data is the frequency response of a 16-μm-thick PSP sample. These data were acquired using the experimental setup of Winslow et al.[10] and Carroll et al.[11] The general uncertainties of the measurements are ± 0.1 kPa for the conventional pressure transducer and $\pm 2\%$ of the reading for the PSP measurements. On the basis of experimental data, a transfer function of the form

$$\tilde{H}(\omega) = \frac{1 + j\omega\tau_1}{1 + j\omega\tau_2} \tag{6}$$

was chosen to model the system. This particular form of transfer function is that of a lag system. The transfer function was applied to the input data, $P_{\text{in}}(t)$, from a high-frequency response pressure transducer, using the MATLAB® computer software to achieve a

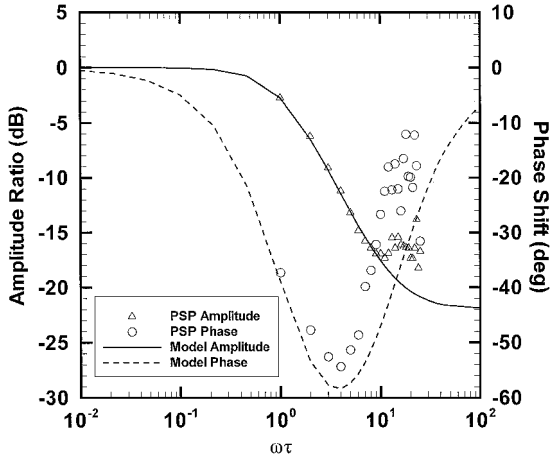

Fig. 2 Frequency response of a 16-μm-thick PSP sample.

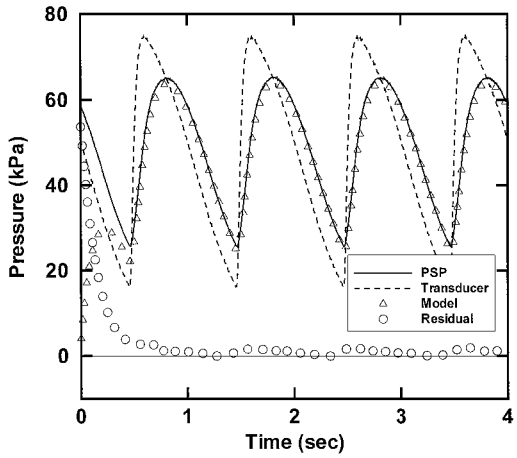

Fig. 3 Comparison of PSP data and empirical model data.

model output pressure, $P_{\text{model}}(t)$. The parameters τ_1 and τ_2 were varied until the root mean square error (RMSE) between the PSP-indicated pressure, $P_{\text{out}}(t)$, and the model output was minimized. The resulting values of τ_1 and τ_2 were 0.012 and 0.15 s, respectively. The model transfer function is also shown in Fig. 2. The time domain data for this experiment are shown in Fig. 3. Shown in Fig. 3 are the PSP-indicated pressure, the pressure measured by the conventional transducer, the model output data, and the residual between the PSP-indicated pressure and the model output. The absolute error between the PSP data and the model output data is less than 2 kPa (RMSE = 0.97 kPa). As can be seen, the transfer function of Eq. (6) does a reasonably good job of approximating the PSP system dynamics. However, the parameters of this curvefit depend on the thickness and chemistry of the PSP layer in an unknown manner. That is, if the thickness or formulation of the PSP was changed, a different transfer function would result. Hence, the empirical approach is useful for a single sample but does not transfer well to the type of experiments one might actually want to perform. Therefore, a more thorough understanding of the physical processes involved in the dynamics of PSP is required.

Diffusion Models

As was mentioned earlier, PSP is based on the fluorescence quenching effect of oxygen on luminescent molecules in a polymer binder. This model tracks the process by which an unsteady pressure above the PSP affects the oxygen distribution within the PSP and in turn causes the intensity of luminescence to change in time.

Under static conditions, the oxygen concentration within the layer will be constant and related to the pressure over the surface via a linear sorption law (Henry's law):

$$n = \sigma P \tag{7}$$

Also under static conditions, the intensity of luminescence is related to the pressure over the surface via a static calibration:

$$I = f(P) \tag{8a}$$

or

$$P = g(I) \tag{8b}$$

due to the luminescence quenching effect of oxygen within the layer. Note here that the functions f and g are inverse functions. For the moment a generic relation between pressure and intensity is assumed. Later, specific forms for the static calibration function will be used to complete the system dynamics. Letting $I^* = I/I_{\text{ref}}$ and $P^* = P/P_{\text{ref}}$, the calibration equation can be brought into a dimensionless form

$$I^* = f(P^*) \tag{9}$$

In the preceding equation, the nondimensional integrated intensity I^* can be replaced by the dimensionless intensity per unit depth, J^*, by noting that

$$I^* = I/I_{\text{ref}} = (I/a)/(I_{\text{ref}}/a) = J/J_{\text{ref}} = J^* \tag{10}$$

Also pressure can be replaced with oxygen concentration by noting that

$$P^* = P/P_{\text{ref}} = \sigma P/\sigma P_{\text{ref}} = n/n_{\text{ref}} = n^* \tag{11}$$

A static calibration equation relating the intensity per unit depth to the oxygen concentration can then be given as

$$J^* = f(n^*) \tag{12}$$

Neglecting any internal light attenuation, this equation also holds on a local level, that is, at any point within the layer.[3] Therefore, Eq. (12) can be used within the layer by considering both J^* and n^* to be functions of depth x. In addition, this equation holds as a function of time, assuming that the kinetics of the quenching process are much faster than the kinetics of the diffusion process. The kinetics of the quenching process are on the order of the lifetime of the fluorescence, which is itself on the order of microseconds for the ruthenium-based paints.[2,12,13] Then, since the kinetics of the diffusion process are on the order of milliseconds to seconds for typical coating thicknesses,[4,9–11] the assumption is indeed valid. Restating Eq. (12) with the new dependencies, one observes that the static calibration provides a dynamic relation between intensity at a given depth within the PSP layer and the oxygen concentration at that depth

$$J^*(x,t) = f\ n^*(x,t)] \tag{13}$$

The next step is to solve for the oxygen concentration as a function of depth and time for a given surface pressure input, $P_{\text{in}}(t) = P(a,t)$. This will be done using the one-dimensional mass diffusion equation with boundary conditions and initial conditions of

$$\frac{\partial^2 n}{\partial x^2} = \frac{1}{D}\frac{\partial n}{\partial t} \tag{14a}$$

$$n(a,t) = \sigma P_{\text{in}}(t) \tag{14b}$$

$$\frac{\partial n(0,t)}{\partial x} = 0 \tag{14c}$$

$$n(x,0) = \sigma P_{\text{in}}(0) \tag{14d}$$

The governing equation (14a) assumes that the PSP layer is infinite in the transverse directions and that the diffusivity is constant. The first boundary condition, Eq. (14b), makes the assumption that the kinetics of the sorption process are much faster than the kinetics of the diffusion process, such that the surface of the PSP is in equilibrium with the air above. The second boundary condition, Eq. (14c), represents a nonpenetration condition at the substrate. The initial condition, Eq. (14d), states that the oxygen concentration across the layer

is initially constant (i.e., in equilibrium initially). Equations (14a–14d) or their underlying assumptions have been used in many other analyses of the solubility and diffusion of gases in polymers.[3,8,10,11,14] These equations can be nondimensionalized by letting $x^* = x/a$, $t^* = t/\tau$, where $\tau \equiv a^2/D$ and making use of Eq. (11) to arrive at

$$\frac{\partial^2 n^*}{(\partial x^*)^2} = \frac{\partial n^*}{\partial t^*} \tag{15a}$$

$$n^*(1, t^*) = P^*_{\text{in}}(t^*) \tag{15b}$$

$$\frac{\partial n^*(0, t^*)}{\partial x^*} = 0 \tag{15c}$$

$$n^*(x^*, 0) = P^*_{\text{in}}(0) \tag{15d}$$

In PSP measurements, the luminescence intensity is the quantity actually measured. Thus, it is instructive to recast Eqs. (15a–15d) in terms of intensity. Inverting Eq. (13) to get $n^*(x^*, t^*) = g\ J^*(x^*, t^*)]$ and substituting into Eqs. (15a–15d) yields

$$\frac{\partial J^*}{\partial t^*} = \frac{\partial^2 J^*}{(\partial x^*)^2} + \frac{\partial^2 g/(\partial J^*)^2}{\partial g/\partial J^*}\left(\frac{\partial J^*}{\partial x^*}\right)^2 \tag{16a}$$

$$J^*(1, t^*) = f\left[P^*_{\text{in}}(t^*)\right] \tag{16b}$$

$$\frac{\partial J^*(0, t^*)}{\partial x^*} = 0 \tag{16c}$$

$$J^*(x^*, 0) = f\left[P^*_{\text{in}}(0)\right] \tag{16d}$$

Equations (16a–16d) represent a nonlinear partial differential equation with nonhomogeneous boundary conditions describing the intensity distribution as a function of depth and time. Notice that recasting the formulation in terms of intensity, J^*, instead of oxygen concentration, n^*, introduces the nonlinear term. The problem can be restated via a change of variables

$$K(x^*, t^*) = J^*(x^*, t^*) - f\left[P^*_{\text{in}}(t^*)\right] \tag{17}$$

to achieve a nonlinear partial differential equation with homogeneous boundary conditions and initial conditions

$$\frac{\partial K}{\partial t^*} = \frac{\partial^2 K}{(\partial x^*)^2} + \frac{\partial^2 g/(\partial J^*)^2}{\partial g/\partial j^*}\left(\frac{\partial K}{\partial x^*}\right)^2 - \frac{\partial f\left[P^*_{\text{in}}(t^*)\right]}{\partial t^*} \tag{18a}$$

$$K(1, t^*) = 0 \tag{18b}$$

$$\frac{\partial K(0, t^*)}{\partial x^*} = 0 \tag{18c}$$

$$K(x^*, 0) = 0 \tag{18d}$$

The output of a PSP measurement is the integrated intensity (neglecting internal absorption)

$$I^*_{\text{out}}(t^*) = \int_0^1 J^*(x^*, t^*)\, dx^* = \int_0^1 K(x^*, t^*)\, dx^* + f\left[P^*_{\text{in}}(t^*)\right] \tag{19}$$

The integrated intensity is then related to the indicated pressure through the static calibration, $P^*_{\text{out}}(t^*) = g\ I^*_{\text{out}}(t^*)]$.

Equations (18a–18d) are an extremely important set of equations, representing the error between the intensity output by the uppermost layer of the PSP and the intensity output from a given depth within the PSP layer. The term on the left-hand side (LHS) and the first term on the right-hand side (RHS) of Eq. (18a) are both linear terms. The last term on the RHS of that same equation is a forcing term. The middle term on the RHS is in general highly nonlinear and contains a forcing part as well. Because of the nonlinearity of this term, it is not possible in general to apply classical controls methods, as will be shown later. With the use of two different assumed calibration functions and modal analysis, a system model now will be developed and simulated.

Diffusion Model with Linear Calibration

The first calibration function to be investigated will be

$$I^* = f(P^*) = c_0 + c_1 P^* \tag{20a}$$

or

$$P^* = g(I^*) = (I^* - c_0)/c_1 \tag{20b}$$

This form of calibration is not typically used in PSP analysis; however, it has one important feature. Using a calibration that is linear between intensity and pressure causes the (normally) nonlinear term from Eq. (18a) to drop out, yielding

$$\frac{\partial K(x^*, t^*)}{\partial t^*} = \frac{\partial^2 K(x^*, t^*)}{(\partial x^*)^2} - \frac{\partial f\left[P^*_{\text{in}}(t^*)\right]}{\partial t^*} \tag{21}$$

which is now a linear partial differential equation with forcing. The solution to this equation will be assumed via separation of variables as

$$K(x^*, t^*) = \sum_{i=1}^{\infty} \alpha_i(t^*)\Psi_i(x^*) \tag{22}$$

where $\Psi_i(x^*)$ are sine or cosine functions. This form of solution is based on a method called modal analysis and is often used in linear systems dynamics modeling. The spatial eigenfunctions $\Psi_i(x^*)$ must satisfy the boundary conditions Eqs. (18b) and (18c)] giving

$$\Psi_i(x^*) = \cos\left(\lambda_i x^*\right) \quad \text{where} \quad \lambda_i = (2i - 1)(\pi/2) \tag{23}$$

Substituting into Eq. (21), multiplying by $\Psi_k(x^*)$, and integrating across the thickness of the layer gives

$$\dot{\alpha}_i(t^*) = -\lambda_i^2 \alpha_i(t^*) - 2\ \sin(\lambda_i)/\lambda_i]\dot{f}\left[P^*_{\text{in}}(t^*)\right] \tag{24}$$

Substituting Eqs. (22) and (23) into Eq. (19) yields the output

$$I^*_{\text{out}}(t^*) = \sum_{i=1}^{\infty} \alpha_i(t^*)\frac{\sin(\lambda_i)}{\lambda_i} + f\left[P^*_{\text{in}}(t^*)\right] \tag{25}$$

In implementation the infinite sum of Eq. (22) will be truncated after some number of terms M. After truncation, Eqs. (24) and (25) can be written in the standard linear systems form

$$\begin{pmatrix} \vdots \\ \dot{\alpha}_i(t^*) \\ \vdots \end{pmatrix} = \begin{bmatrix} \ddots & 0 & 0 \\ 0 & -\lambda_i^2 & 0 \\ 0 & 0 & \ddots \end{bmatrix} \begin{pmatrix} \vdots \\ \alpha_i(t^*) \\ \vdots \end{pmatrix} + \begin{bmatrix} \vdots & \vdots \\ 0 & -2\sin(\lambda_i)/\lambda_i \\ \vdots & \vdots \end{bmatrix} \begin{pmatrix} f\left[P^*_{\text{in}}(t^*)\right] \\ \dot{f}\left[P^*_{\text{in}}(t^*)\right] \end{pmatrix} \tag{26a}$$

$$I^*_{\text{out}}(t^*) = \left(\cdots, \frac{\sin(\lambda_i)}{\lambda_i}, \cdots\right) \begin{pmatrix} \vdots \\ \alpha_i(t^*) \\ \vdots \end{pmatrix} + (1, 0) \begin{pmatrix} f\left[P^*_{\text{in}}(t^*)\right] \\ \dot{f}\left[P^*_{\text{in}}(t^*)\right] \end{pmatrix} \tag{26b}$$

This system is a multi-input, single-output system with inputs of $f\ P^*_{\text{in}}(t^*)]$ and $\dot{f}\ P^*_{\text{in}}(t^*)]$, state vector $\alpha_i(t^*)$, and output $I^*_{\text{out}}(t^*)$. A useful property of this model is that the system matrix is diagonal with distinct, nonzero eigenvalues. The usefulness of this property is in calculating the observability and controllability matrices. It can be shown that these matrices are both full rank, thus implying that

Table 1 Sample PSP indicated pressures

$P^*_{\text{in}}(t^*)$	$P^*_{\text{out}}(t^*)$
$P^*_0 + P^*_1 \text{step}(t^*)$	$P^*_0 + P^*_1 \left\{ 1 - \frac{8}{\pi^2} \sum_{m=1}^{\infty} \left(\frac{1}{2m-1} \right)^2 \exp\left[-(2m-1)^2 \frac{\pi^2}{4} t^* \right] \right\}$
$P^*_0 + P^*_1 \sin(\omega^* t^*)$	$P^*_0 + P^*_1 \frac{\tanh(\beta)}{\beta} \sin(\omega^* t^*), \beta = \sqrt{j\omega^*}, \quad \omega^* = \omega\tau$

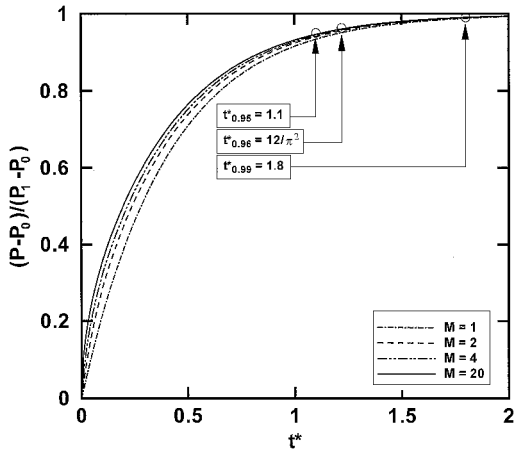

Fig. 4 Simulated PSP unit step response using diffusion-based model with a linear calibration.

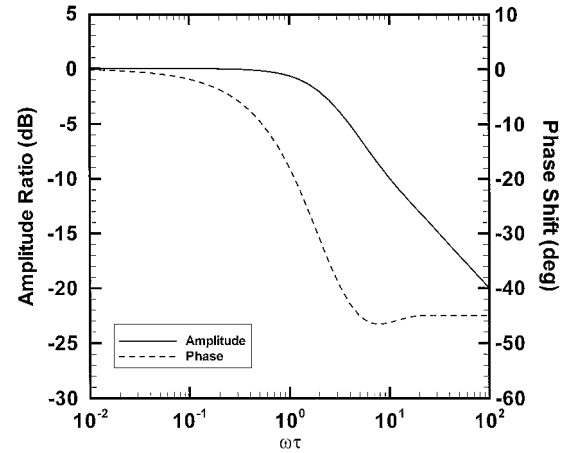

Fig. 5 Simulated PSP frequency response using diffusion-based model with a linear calibration.

the system is both observable and reachable. These two properties should allow a simple compensator to be constructed. There is one additional point of interest concerning this system. Because it is a linear system and the relation between intensity and pressure is linear, Eqs. (26a) and (26b) can be rewritten via a linear transformation as a system between the input pressure and the indicated output pressure:

$$\begin{pmatrix} \vdots \\ \dot{\alpha}_i(t^*) \\ \vdots \end{pmatrix} = \begin{bmatrix} \ddots & 0 & 0 \\ 0 & -\lambda_i^2 & 0 \\ 0 & 0 & \ddots \end{bmatrix} \begin{pmatrix} \vdots \\ \alpha_i(t^*) \\ \vdots \end{pmatrix} + \begin{bmatrix} \vdots & \vdots \\ 0 & -2\sin(\lambda_i)/\lambda_i \\ \vdots & \vdots \end{bmatrix} \begin{pmatrix} P^*_{\text{in}}(t^*) \\ \dot{P}^*_{\text{in}}(t^*) \end{pmatrix} \tag{27a}$$

$$P^*_{\text{out}}(t^*) = \left(\cdots, \frac{\sin(\lambda_i)}{\lambda_i}, \cdots \right) \begin{pmatrix} \vdots \\ \alpha_i(t^*) \\ \vdots \end{pmatrix} + (1, 0) \begin{pmatrix} P^*_{\text{in}}(t^*) \\ \dot{P}^*_{\text{in}}(t^*) \end{pmatrix} \tag{27b}$$

It can be shown that this output is identical to the solution for $n^*(x^*, t^*)$ integrated across the layer, that is

$$P^*_{\text{out}}(t^*) = \int_0^1 n^*(x^*, t^*)\, dx^* \tag{28}$$

where $n^*(x^*, t^*)$ is obtained by solution of Eqs. (15a–15d). This system is then identical to that used by Carroll et al.[11] For a number of inputs $P^*_{\text{in}}(t^*)$, the output from the system is analytic. Table 1 below lists several of these solutions.[15]

Note that the function step(t), sometimes referred to as the unit step function, is zero for $t < 0$ and unity for $t > 0$. Also note that the solution shown for the sinusoidal input is only that due to the steady periodic conditions, not the initial transient period.

Shown in Fig. 4 is the simulated step response using the first 1, 2, 4, and 20 terms from the analytical solution of Table 1. The responses of the first three curves have been renormalized so as to approach unity as time grows large. Labeled on the graph are several points throughout the response. It can be seen that the time to reach 99% of the total response is approximately 1.80τ, compared with the value of $(12/\pi^2)\tau$ put forth in the paper by Borovoy et al.[5] It can also be seen that a model order of $M = 5$ should be sufficient to represent most of the dynamic behavior.

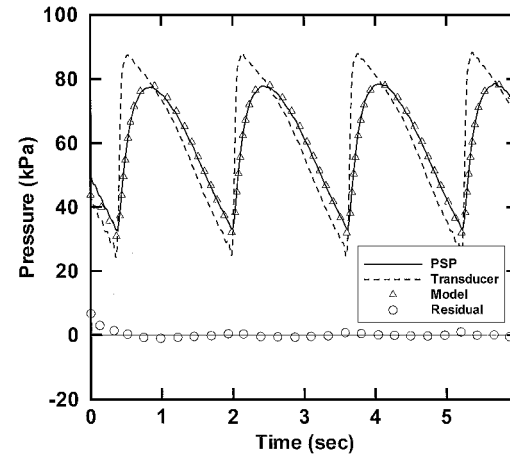

Fig. 6 Comparison of PSP data and diffusion-based model output with a linear calibration.

Figure 5 shows the simulated frequency response of the PSP. There are two interesting items of note here. First, the amplitude slopes off at −10 dB/decade. Second, the phase shift levels off at −45°. Following the trend of first- and second-order systems, it would then seem that this system exhibits the behavior of a half-order system, which has some meaning in the context of fractional calculus, in which derivatives and integrals of rational order are defined. In the text by Oldham and Spanier[16] on this subject, the relation between many diffusion-based phenomena and the half-order derivative or semiderivative is shown. An attempt has been made to express this current model using fractional calculus, but no clear results have yet been achieved.

Figure 6 shows a set of experimental input and output pressure data. Also included in Fig. 6 is the model output pressure based on

the linearized diffusion model of Eqs. (27a) and (27b), with $M = 5$. The value of the time constant that minimizes the RMSE between the PSP-indicated pressure and the model output pressure is $\tau = 0.437$. The RMSE of the curvefit is 0.91 kPa, which is a very good fit. The thickness of this particular sample was 17 μm. Using $\tau \equiv a^2/D$ a value of $D = 6.6 \times 10^{-6}$ cm^2/s is acquired for the mass diffusivity.

An equivalent form of the model of Eqs. (27a) and (27b) has been shown to adequately represent experimental data.[8] One interesting application of this model was that of Carroll et al.[11] In this work, the model was applied to experimental data using numerical convolution and nonlinear least-squares curve fitting to calculate the time constant τ. The thickness, a, of the PSP was then measured using an eddy current gauge. Once these two values had been found, the mass diffusivity could then be calculated via $\tau \equiv a^2/D$ or $D = a^2/\tau$. The values of mass diffusivity found ranged from 4.99×10^{-5} cm^2/s at 10 °C to 7.62×10^{-5} cm^2/s at 40 °C. Using an Arrhenius model of the form

$$D = A \exp(-E/RT) \tag{29}$$

to fit the temperature data a value of 2.48 kcal/mole was found for the activation energy. These values of mass diffusivity and activation energy were in excellent agreement with similar values from other sources.[3,13,17] Hence, it was shown that the simple linear model could be used in a diagnostic manner to determine various physical properties of the PSP.

Diffusion Model with Linear Stern–Volmer Calibration

The most widely used calibration for PSP is based on the Stern–Volmer relation. It may be expressed as a linear relation between pressure and the inverse of intensity:

$$I^* = f(P^*) = 1/\ b + (1-b)P^*] \tag{30a}$$

or

$$P^* = g(I^*) = \ (1/I^*) - b]/(1-b) \tag{30b}$$

In these equations, b is the intercept of the standard linear Stern–Volmer relation and $1-b$ is the slope. Applying Eq. (10) to Eqs. (30a) and (30b) and substituting into Eq. (18a) gives

$$\frac{\partial K}{\partial t^*} = \frac{\partial^2 K}{(\partial x^*)^2} - \frac{2}{K + f\left[P^*_{\text{in}}(t^*)\right]}\left(\frac{\partial K}{\partial x^*}\right)^2 - \frac{\partial f\left[P^*_{\text{in}}(t^*)\right]}{\partial t^*} \tag{31}$$

This is the governing equation for the PSP dynamics based on the linear Stern–Volmer calibration. It can be seen that the middle term on the RHS is highly nonlinear and contains a forcing component as well. Because of this term, a numerical solution to this equation would require a complex numerical algorithm. However, rather than perform a direct solution to this equation, a different method will be employed. It will begin by solving for the oxygen concentration from Eqs. (15a–15d). These equations can be transformed to a linear partial differential equation with forcing with homogeneous boundary conditions and initial condition via

$$m(x^*, t^*) = n^*(x^*, t^*) - P^*_{\text{in}}(t^*) \tag{32}$$

Then, modal analysis can be applied see Eqs. (22) and (23)]. The resulting system equation is identical to Eq. (27a). The system equation together with an output equation designed to give the oxygen concentration distribution is then

$$\begin{pmatrix} \vdots \\ \dot{\alpha}_i(t^*) \\ \vdots \end{pmatrix} = \begin{bmatrix} \ddots & 0 & 0 \\ 0 & -\lambda_i^2 & 0 \\ 0 & 0 & \ddots \end{bmatrix} \begin{pmatrix} \vdots \\ \alpha_i(t^*) \\ \vdots \end{pmatrix} + \begin{bmatrix} \vdots & \vdots \\ 0 & -2\sin(\lambda_i)/\lambda_i \\ \vdots & \vdots \end{bmatrix} \begin{pmatrix} P^*_{\text{in}}(t^*) \\ \dot{P}^*_{\text{in}}(t^*) \end{pmatrix} \tag{33a}$$

$$n^*(x^*, t^*) = \left(\cdots, \cos\left(\lambda_i x^*\right), \cdots\right) \begin{pmatrix} \vdots \\ \alpha_i(t^*) \\ \vdots \end{pmatrix} + (1, 0) \begin{pmatrix} P^*_{\text{in}}(t^*) \\ \dot{P}^*_{\text{in}}(t^*) \end{pmatrix} \tag{33b}$$

This system is linear and can be easily solved at a discrete number of points throughout the layer to achieve an oxygen concentration distribution. This oxygen concentration distribution will then be converted to an intensity distribution by using the calibration in a dynamic sense:

$$J^*(x^*, t^*) = 1/\ b + (1-b)n^*(x^*, t^*)] \tag{34}$$

It may be helpful for the reader to refer once again to the discussion leading from Eq. (9) up to Eq. (13) for the validity of Eq. (34). Then, the intensity distribution can be numerically integrated to get the integrated intensity output. Making use of the static calibration of Eq. (30b) achieves the indicated output pressure.

Figures 7 and 8 show the simulated response of PSP to a positive and a negative step in pressure, respectively. For the positive step, the initial pressure was $P^*_0 = 0.1$, the final pressure was $P^*_1 = 1.0$, and the intercept of the linear Stern–Volmer calibration was $b = 0.2$. For the negative step, the values of P^*_0 and P^*_1 were reversed. Shown in Figs. 7 and 8 are comparisons of the two models, based on the linear calibration and the linear Stern–Volmer calibration, respectively. For the datasets based on the linear calibration, a model order of $M = 5$ was used. For the data based on the linear Stern–Volmer calibration, a model order of $M = 5$ was used to calculate the oxygen concentration distribution. This was evaluated at 21 evenly spaced grid points throughout the depth of the layer. Next, it was converted to intensity per unit depth via the calibration equation and numerically integrated across the layer using the trapezoidal rule

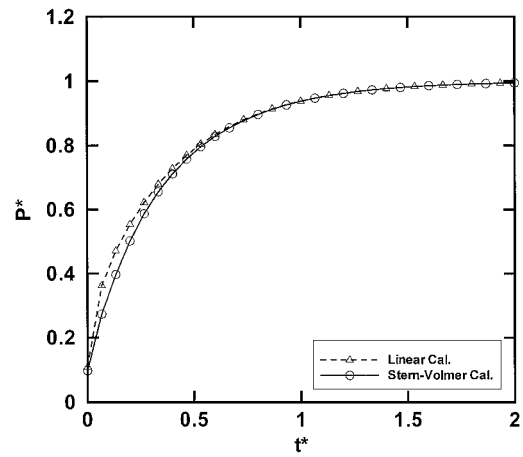

Fig. 7 Simulated positive step in pressure (model comparison).

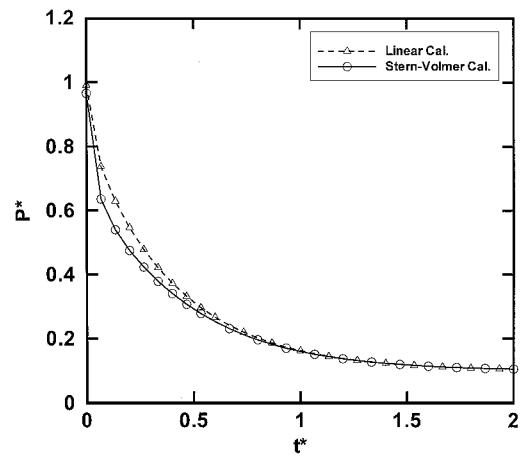

Fig. 8 Simulated negative step in pressure (model comparison).

Table 2 Comparison of curvefits

Calibration	τ, s	RMSE, kPa
Linear	1.25	4.10
Linear Stern–Volmer	1.11	1.39

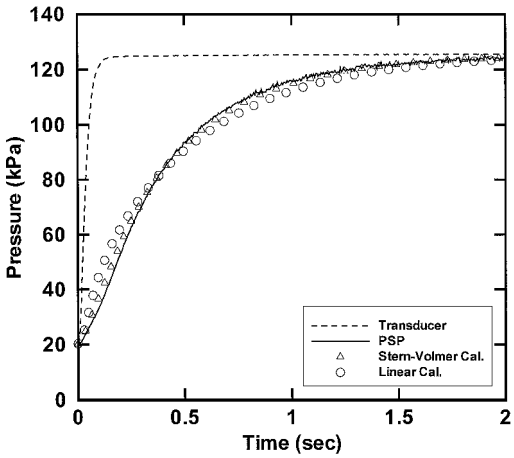

Fig. 9 Positive step in pressure (model comparison).

integrator. The integrated intensity was then converted to an indicated pressure by means of the calibration. From Fig. 7 it can be seen that for a positive step in pressure, the linear model solution leads the linear Stern–Volmer model solution. In Fig. 8 this behavior is reversed. There are several items of note with respect to these comparisons. First, the difference between the models is a function of each of the values P_0^*, P_1^*, and b. If the pressure data were scaled via $(P^* - P_0^*)/(P_1^* - P_0^*)$ the response of the linear Stern–Volmer-based model would continue to show different behavior for different values of P_0^*, P_1^*, and b, whereas the linear calibration-based model would always show the same response. Second, as ΔP of the step decreases, the two models will collapse to the same behavior. Similarly, the models will also collapse to the same behavior for $b \to 1$.

Figure 9 shows experimental input and output data for a positive step in pressure. Also shown is a comparison of curvefits of the two preceding diffusion-based models. The results of the curvefits are shown in Table 2. For the model based on the linear Stern–Volmer calibration, an intercept of $b = 0.14$ was used. It is quite clear that the model using the linear Stern–Volmer calibration does a much better job of approximating the PSP response than the model based on the linear calibration.

Conclusions

A brief history of PSP in unsteady conditions has been presented. The lack of an entirely physical model for the PSP behavior was shown to exist in the literature. With this in mind two models were presented. The first contained absolutely no physics and was based entirely on curvefitting an empirical equation to the input/output data. This model works well, as long as parameters such as PSP thickness, composition, and temperature remain constant. Because it is in general not feasible to keep these parameters constant, a more fundamental model is needed. The second was based on the one-dimensional mass diffusion equation and an assumed form for the static calibration function. Two forms for the static calibration were presented along with their effect on the system dynamics. The first calibration function was a simple linear relationship between pressure and intensity. The system model using this calibration function could be stated in the form of a system of linear equations and was easy to implement. The second calibration function was the standard linear Stern–Volmer calibration often used in PSP testing. The system model under this calibration function was shown to have a nonlinear term that could not be handled using conventional linear systems techniques. This led to the development of an alternate solution method, wherein the oxygen concentration within the PSP layer was acquired first. Then, this oxygen concentration distribution was converted to intensity distribution by means of the static calibration. The intensity distribution was then integrated across the layer to achieve the integrated intensity from the PSP. Finally, the integrated intensity was converted to pressure via the static calibration. The diffusion-based model using a linear Stern–Volmer calibration function was shown to more accurately model the PSP response than the diffusion-based model using a linear calibration. However, the diffusion-based models were shown to have similar characteristics in general. All of the models presented were shown to adequately represent experimental data. Additional diffusion-based models can easily be derived by using alternate calibration functions, for example, a quadratic Stern–Volmer calibration. Now that models for the dynamic behavior of PSP have been developed, the task of designing a compensator can begin. This will be the topic of a forthcoming paper. To be able to use PSP in a full dynamic sense would represent a major step forward in the evolution of PSP as a measurement technique.

Acknowledgment

We thank Wim Ruyten of Sverdrup Technology/AEDC Group for insightful comments in the development of the diffusion-based model.

References

[1]McLachlan, B. G., and Bell, J. H., "Pressure-Sensitive Paint in Aerodynamic Testing," *Experimental Thermal and Fluid Science*, Vol. 10, 1995, pp. 470–485.

[2]Liu, T., Campbell, B. T., Burns, S. P., and Sullivan, J. P., "Temperature- and Pressure-Sensitive Luminescent Paints in Aerodynamics," *Applied Mechanics Review*, Vol. 50, No. 4, 1997, pp. 227–246.

[3]Cox, M. E., and Dunn, B., "Oxygen Diffusion in Poly(dimethyl Siloxane) using Fluorescence Quenching. I. Measurement Technique and Analysis," *Journal of Polymer Science Part A: Polymer Chemistry*, Vol. 24, 1986, pp. 621–636.

[4]Baron, A. E., Danielson, J. D. S., Gouterman, M., Wan, J. R., Callis, J. B., and McLachlan, B., "Submillisecond Response Times of Oxygen-Quenched Luminescent Coatings," *Review of Scientific Instruments*, Vol. 64, No. 12, 1993, pp. 3394–3402.

[5]Borovoy, V., Bykov, A., Mosharov, V., Orlov, A., Radchenko, V., and Phonov, S., "Pressure Sensitive Paint Application in Shock Wind Tunnel," *16th ICIASF Record*, IEEE-95CH34827, 1995, pp. 34.1–34.4.

[6]Engler, R. H., "Further Developments Of Pressure Sensitive Paint (OPMS) for Non Flat Models in Steady Transonic Flow and Unsteady Conditions," *16th ICIASF Record*, IEEE-95CH34827, 1995, pp. 33.1–33.8.

[7]Carroll, B. F., Winslow, N., Abbitt, J., Schanze, K., and Morris, M., "Pressure Sensitive Paint: Application to a Sinusoidal Pressure Fluctuation," *16th ICIASF Record*, IEEE-95CH34827, 1995, pp. 35.1–35.6.

[8]Carroll, B. F., Abbitt, J. D., Lukas, E. W., and Morris, M. J., "Step Response of Pressure-Sensitive Paints," *AIAA Journal*, Vol. 34, No. 3, 1996, pp. 521–526.

[9]Hubner, J., Carroll, B., Schanze, K., Ji, H., and Holden, M., "Temperature-and Pressure-Sensitive Paint Measurements in Short-Duration Hypersonic Flow," AIAA Paper 99-0388, 1999.

[10]Winslow, N. A., Carroll, B. F., and Setzer, F. M., "Frequency Response of Pressure Sensitive Paints," AIAA Paper 96-1967, 1996.

[11]Carroll, B., Winslow, N., and Setzer, F., "Mass Diffusivity of Pressure Sensitive Paints via System Identification," AIAA Paper 97-0771, 1997.

[12]Burns, S. P., and Sullivan, J. P., "The Use of Pressure Sensitive Paints on Rotating Machinery," *16th ICIASF Record*, IEEE-95CH34827, 1995, pp. 32.1–32.14.

[13]Schanze, K. S., Carroll, B. F., Korotkevitch, S., and Morris, M. J., "Temperature Dependence of Pressure Sensitive Paints," *AIAA Journal*, Vol. 35, No. 2, 1997, pp. 306–310.

[14]Evnochides, S. K., and Henley, E. J., "Simultaneous Measurement of Vapor Diffusion and Solubility Coefficients in Polymers by Frequency Response Techniques," *Journal of Polymer Science Part A-2*, Vol. 8, 1970, pp. 1987–1997.

[15]Carslaw, H. S., and Jaeger, J. C., *Conduction of Heat in Solids*, Oxford Univ. Press, London, 1959.

[16]Oldham, K. B., and Spanier, J., *The Fractional Calculus*, Academic Press, New York, 1974.

[17]Pauly, S., "Permeability and Diffusion Data," *Polymer Handbook*, 3rd ed., edited by J. Brandrup and E. H. Immergut, Wiley-Interscience, New York, 1989, pp. VI/435–VI/449.

R. P. Lucht
Associate Editor